JOURNAL OF CHEMICAL & ENGINEERING DATA

ARTICLE

pubs.acs.org/jced

Solid−Liquid Equilibrium of Binary Mixtures Containing Fatty Acids and Triacylglycerols

Mariana C. Costa,[†] Laslo A. D. Boros,[‡] Jackiney A. Souza,[‡] Marlus P. Rolemberg,[§] Maria A. Krähenbühl,[‡] and Antonio J. A. Meirelles*[,†]

[†]EXTRAE, Department of Food Engineering, Faculty of Food Engineering (DEA-FEA), University of Campinas (UNICAMP), Postal code: 13083-862, Campinas, São Paulo, Brazil

[‡]LPT, Department of Chemical Processes, School of Chemical Engineering (DPQ-FEQ), University of Campinas (UNICAMP), Postal code: 13083-970, Campinas, São Paulo, Brazil

[§]DETQUI, Department of Chemical Technology, Federal University of Maranhão (UFMA), São Luís, Maranhão, Brazil

ABSTRACT: Solid−liquid phase diagrams of the following systems were measured using differential scanning calorimetry (DSC): tristearin (2,3-di(octadecanoyloxy)propyl octadecanoate) + tripalmitin (2,3-di(hexadecanoyloxy)propyl hexadecanoate), tristearin (2,3-di(octadecanoyloxy)propyl octadecanoate) + palmitic acid (*n*-hexadecanoic acid), tristearin (2,3-di(octadecanoyloxy)propyl octadecanoate) + linoleic acid (*cis*-9,*cis*-12-octadecadienoic acid), tripalmitin (2,3-di(hexadecanoyloxy)propyl hexadecanoate) + triolein (2,3-bis[[(*Z*)-octadec-9-enoyl]oxy]propyl (*Z*)-octadec-9-enoate), and tripalmitin (2,3-di(hexadecanoyloxy)propyl hexadecanoate) + commercial oleic acid (commercial (*Z*)-octadec-9-enoic acid). The eutectic point was observed for two systems, tristearin with tripalmitin or with palmitic acid. Polarized optical microscopy was employed to investigate the solid phase of the systems and confirmed the occurrence of a solid solution at the extreme of the phase diagram rich in the component with a higher melting temperature. Margules-2-suffix, Margules-3-suffix, nonrandom two-liquid (NRTL), and universal quasichemical functional group activity coefficient (UNIFAC) models were employed to describe the liquidus line of the studied systems, except for the system formed by tripalmitin (2,3-di(hexadecanoyloxy)propyl hexadecanoate) + commercial oleic acid (commercial (*Z*)-octadec-9-enoic acid) which is a pseudobinary system that was well-described by the UNIFAC model. The best results for the other systems were obtained when employing the Margules-3-suffix and NRTL models.

INTRODUCTION

The importance of vegetable oils and fats in the human diet and in a series of products of the pharmaceutical and chemical industries is well-known. However, with the growth of the oleochemical industry, principally based on the biodiesel production, industry profits may further increase if byproducts generated along the different stages of oil processing, should they be rich in fatty acids, triacylglycerols and so on, were utilized for producing substances of high added value. Therefore, it is important to know the phase behavior of such substances to solve problems related to their separation and purification processes.

Studies on the solid−liquid equilibrium (SLE) of vegetable oils and fat components are not so often published in the literature,[1,2] where the most common data reported are related to mixtures containing fatty acids and organic solvents.[3−5] More recently data have been published for systems formed by triacylglycerols,[6,7] fatty acids,[8,9] and triacylglycerol plus fatty acids.[10] The present study is part of a series of works developed by our research group on the SLE of fatty mixtures.[8−15] This study reports SLE data of the following systems: tristearin + tripalmitin, tristearin + palmitic acid, tristearin + linoleic acid, tripalmitin + triolein, and tripalmitin + commercial oleic acid. The experimental data were measured by differential scanning calorimetry (DSC) and modeled using Margules-2-suffix, Margules-3-suffix, nonrandom two-liquid (NRTL), and universal quasichemical functional group activity coefficient (UNIFAC) equations.

Prior studies on these systems found in the literature are focused on the polymorphic transitions of tristearin and tripalmitin[16−20] or on the crystallization kinetics of tristearin, tripalmitin, and their mixtures with triolein.[21] Such studies presented a detailed description of the polymorphic forms of these compounds, but the experimental conditions employed are different, so that a quantitative comparison of the results is not viable.

The phase diagrams reported in this work have not yet been published. These data give a complete description of the liquidus line and also of some transitions observed beneath this line, as well as they reveal the existence of a solid solution at the extremity of the phase diagram rich in the component with a higher melting point. In summary, the experimental data presented here could be used for developing as well as optimizing separation processes applied to these substances. Furthermore, the availability of these data may allow the understanding of the phase equilibrium behavior of such systems.

EXPERIMENTAL SECTION

Reagents. The DSC was calibrated using the following standards: indium (0.9999 mol fraction, TA Instruments; CAS

Received: January 10, 2011
Accepted: June 19, 2011
Published: July 13, 2011

Table 1. Fatty Acids and Triacylglycerols Employed in This Study

reagent	purity	CAS registry no.	supplier
n-hexadecanoic acid (palmitic acid)	min 0.99	57-10-3	Sigma-Aldrich
cis-9,*cis*-12-octadecadienoic acid (linoleic acid)	0.99	60-33-3	Sigma
commercial (*Z*)-octadec-9-enoic acid (commercial oleic acid)			Merck
2,3-di(hexadecanoyloxy)propyl hexadecanoate (tripalmitin)	min 0.99	555-44-2	Nu-Chek
2,3-di(octadecanoyloxy)propyl octadecanoate (tristearin)	min 0.99	555-43-1	Sigma
2,3-bis[[(*Z*)-octadec-9-enoyl]oxy]propyl (*Z*)-octadec-9-enoate (triolein)	min 0.99	122-32-7	Sigma

Table 2. Solid−Liquid Equilibrium Data for the Tristearin + Tripalmitin System

DSC data								optical microscopy data		
$x_{tripalmitin}$	$T_{melting}$/K	$T_{eutectic}$/K	transition temperatures/K					$x_{tripalmitin}$	$T_{start\ melting}$/K	$T_{final\ melting}$/K
0.0000	345.76		332.33	328.26		329.53		0.0000	345.25	346.15
0.1038	344.81		331.22	321.22	332.39	327.19		0.0951	343.95	345.35
0.1992	344.09		331.47	318.73	332.33	325.77		0.2005	342.25	344.75
0.3045	343.19	335.64	331.39	318.68	332.38	324.73		0.2922	337.75	344.35
0.4003	342.23	335.72	331.00	318.58	332.18	323.70		0.4028	336.25	343.55
0.4994	341.12	335.67	329.92	318.45	331.73	322.75		0.4881	336.25	342.35
0.5997	339.70	335.62	329.32	318.37	330.96	321.51	325.64	0.5998	335.25	341.65
0.6497	338.84	335.71	329.17	318.36	330.55	320.90	325.47	0.6789	335.75	337.35
0.7000	335.97		328.98	318.39	330.27	320.50	325.30	0.7895	335.35	337.65
0.7503	336.23		328.71	318.44	329.97	320.08	325.43	0.8936	335.75	338.35
0.7992	336.69	335.93	328.13	318.39	329.41	319.55	324.89	0.9486	336.35	338.75
0.8492	337.22	335.78		318.55		319.36	324.38	1.0000	338.35	339.25
0.9010	337.68	335.23		318.29		319.07	323.14			
1.0000	338.82			318.42		319.10	320.62			

Registry No.: 7440-74-6), benzoic acid (min 0.999 mol fraction, Metler; CAS Registry No.: 65-85-0), and deionized water (Milli-Q, Millipore). The fatty acid and triacylglycerol suppliers and purities are shown in Table 1. All of these substances were used with no further purification.

Methods. The fatty acid composition of commercial oleic acid was determined by gas chromatography of fatty acid methyl esters according to the American Oil Chemists' Society (AOCS) official method (1−62).[22] Commercial oleic acid was prepared in the form of fatty acid methyl esters according to the Hartman and Lago methodology,[23] and the corresponding composition results were published by Rodrigues and co-workers.[24] Fatty mixtures, used in the DSC, were prepared by gravimetry and analyzed in a heating run, after utilizing a thermal treatment to erase thermal memories, at a rate of 0.017 $K \cdot s^{-1}$, as described in previous studies.[8,12,14,25] The experimental uncertainty was estimated based on repeated runs performed with indium and some selected fatty acid samples, and the obtained value was estimated as not higher than 0.3 K.

Table 3. Solid−Liquid Equilibrium Data for the Tristearin + Palmitic Acid System

$x_{palmitic\ acid}$	$T_{melting}$/K	$T_{eutectic}$/K	$T_{exo\ trans}$/K	transition temperatures/K			
0.0000	345.76		329.53			328.26	332.33
0.0580	345.29		330.08		327.80		
0.1463	344.75		328.99	323.68	326.92		
0.2325	344.35	332.24	327.65	323.83			
0.2998	344.07	332.59	327.34	324.03			
0.3997	343.31	332.85	326.98	323.97			
0.5004	342.36	333.00	326.42	323.81			
0.5999	341.31	333.20	326.21	323.57			
0.6992	340.08	333.40	325.45	323.22			
0.7989	337.74	333.42	324.31	323.22			
0.8999	334.02		324.04	322.93			
0.9510	334.48		323.74	322.84			
1.0000	335.44						

RESULTS AND DISCUSSION

The peak top temperature of each thermal event, melting and transitions under the liquidus line, of the five studied systems were determined and are presented in Tables 2 to 6. Figure 1 presents the phase diagram of the system tristearin + tripalmitin determined by the DSC technique and also by optical microscopy. Figure 2 presents the phase diagrams of the systems tristearin + palmitic acid and tristearin + linoleic acid. The phase diagrams of the tripalmitin + triolein and tripalmitin + commercial oleic acid systems are shown in Figure 3. In Figures 1 and 2a there is an eutectic point at the compositions of $x_{tripalmitin} \cong 0.70$ and $x_{tripalmitin} \cong 0.90$, respectively. In the systems formed by tristearin + linoleic acid, tripalmitin + triolein, and tripalmitin + commercial oleic acid (Figures 2b, 3a, and 3b, respectively), the saturated triacylglycerol (tristearin or tripalmitin) remains in the solid state after melting of the second component of each mixture (linoleic acid, triolein, or commercial oleic acid), that is, the

Table 4. Solid−Liquid Equilibrium Data for the Tristearin + Linoleic Acid System

$x_{\text{linoleic acid}}$	T_{fus}/K	$T_{\text{linoleic melting}}$/K	$T_{\text{exo trans}}$/K	transition temperatures/K	
0.0000	345.76		329.53	332.33	328.26
0.1235	345.29		319.50		
0.2076	344.84		309.53		
0.3078	344.31	263.57			
0.3977	343.84	263.81			
0.4976	343.01	263.86			
0.6032	342.06	264.45			
0.7013	341.00	264.98			
0.8010	338.98	267.15			
0.9019	334.77	267.49			
0.9910	323.73	266.39			
1.0000	267.83				

Table 5. Solid−Liquid Equilibrium Data for the Tripalmitin + Triolein System

x_{triolein}	T_{fus}/K	$T_{\text{triolein melting}}$/K	transition temperatures/K		
0.0000	338.82		318.42	319.10	320.62
0.1141	338.29	273.9			
0.2072	337.84	274.61			
0.3038	337.31	276.02			
0.4041	336.47	277.72			
0.5013	335.45	277.89			
0.5985	334.03	278.06			
0.7011	332.15	278.15			
0.8002	329.78	278.15			
0.9005	326.02	278.40			
1.0000	279.22				260.60

component that presents the lower melting temperature. This behavior is the same already described for systems composed of refined rice bran and palm oils with tristearin.[26] This may explain the transition observed in the three mentioned systems around (265, 275, and 280) K, respectively. These temperatures are approximately the melting temperatures of the pure components, indicating the melting of such substances.

Thermograms of the tristearin + tripalmitin system are presented in Figure 4. Figure 4 parts a and g show the thermograms of pure tripalmitin and tristearin, respectively. Both thermograms of pure compounds are in good agreement with those found in the literature,[16,18] and each one presents four peaks, two endothermic and two exothermic ones. In the thermogram of pure tripalmitin (Figure 4g) the first peak, occurring at a lower temperature, represents the melting of the α-form, followed by the polymorphic transition and recrystallization into the β-form, events indicated by the two exothermic peaks.[18] The last peak, at a higher temperature, represents the complete melting of tripalmitin. In the case of tristearin the authors[18] suggest that the two exothermic peaks represent the formation and melting of the β'-form, followed by its recrystallization into the β-form.

It is possible to note in the thermograms presented in Figure 4 that the increase of tripalmitin concentration causes a gradual decrease of the melting temperature until reaching the composition of $x_{\text{tripalmitin}} \cong 0.70$ (Figure 4e), approximately the eutectic

Table 6. Solid−Liquid Equilibrium Data for the Tripalmitin + Commercial Oleic Acid System

$x_{\text{com.oletic acid}}$	T_{fus}/K	$T_{\text{com.oleic melting}}$/K		transition temperatures/K		
0.0000	338.82				318.42	319.10	320.62
0.2875	337.49	281.78	291.78	276.97		
0.4988	335.38	281.66	286.58	277.33		
0.6990	333.97	281.63	287.3	276.98		
0.7998	331.39	281.63	288.27			
0.8497	330.01	281.59	288.35			
0.8981	327.71	281.67	288.29			
0.9402	324.92	282.03	287.53			
0.9706	320.56	281.64	287.19			
1.0000	281.92		247.69			

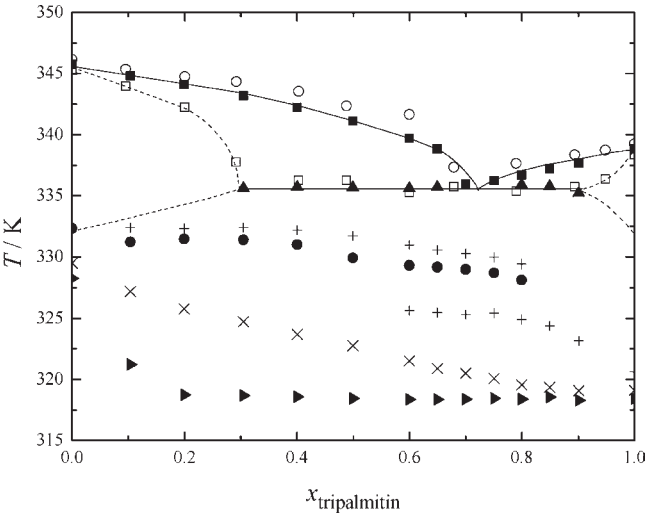

Figure 1. Phase diagram of the tristearin + tripalmitina system. Open symbols (□ and ○) are related to the optical microscopy images, and closed symbols represent the data obtained by DSC: □, beginning of melting temperature; ○, final melting temperature; ■, melting temperature; ▲, eutectic temperature; right-pointing triangle, ×, +, ● transitions in solid phase. Solid lines represent the liquidus line and the eutectic temperature; dashed lines represent the probable boundaries between the solid solution regions and the regions of solid−solid equilibrium (under the eutectic temperature) or SLE (above the eutectic temperature).

point concentration. With the increase of the tripalmitin concentration to $x_{\text{tripalmitin}} \cong 0.80$ (Figure 4f), the temperature required for complete mixture melting increases again.

Tristearin + tripalmitin and tristearin + palmitic acid systems exhibit eutectic points approximately at (336 and 333) K, respectively. In both systems the transitions attributed to the eutectic reaction, represented in the phase diagram by the symbol ▲, are observed for compositions greater than $x_{\text{tripalmitin}} \cong 0.30$ and $x_{\text{palmitic acid}} \cong 0.23$, respectively, as can be seen in Figures 1 and 2a. This is an indication of the solid solution formation at the extremity of the phase diagram rich in tristearin. This will be further discussed below.

In the case of the other three systems studied, tristearin + linoleic acid, tripalmitin + triolein, and tripalmitin + commercial oleic acid, a transition in a temperature very close to the melting temperature of the pure light component was observed in almost

dx.doi.org/10.1021/je200033b |J. Chem. Eng. Data 2011, 56, 3277–3284

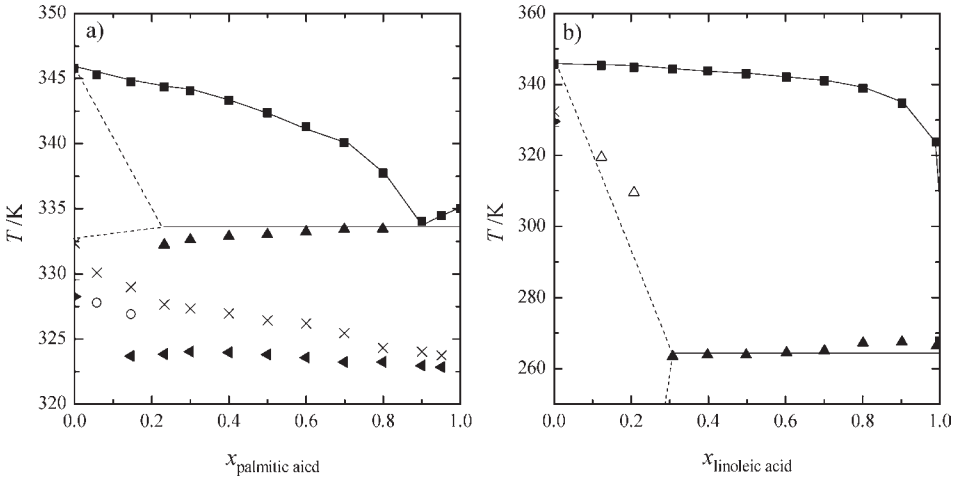

Figure 2. Phase diagram of the (a) tristearin + palmitic acid and (b) tristearin + linoleic acid systems. ■, melting temperature; ▲, eutectic temperature; △, solid−liquid transition; right-pointing triangle, ○, left-pointing triangle, +, × transitions in the solid phase. Solid lines represent the liquidus line and the eutectic temperature; dashed lines represent the probable boundaries between the solid solution region and the regions of solid−solid equilibrium (under the eutectic temperature) or SLE (above the eutectic temperature).

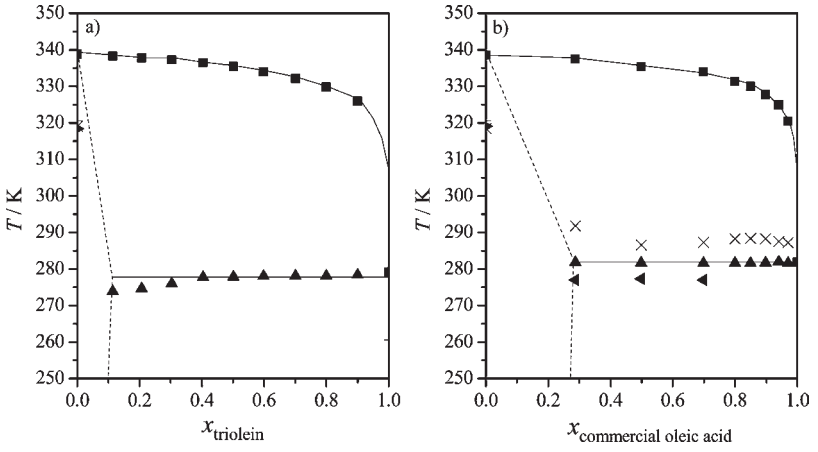

Figure 3. Phase diagram of the (a) tripalmitin + triolein and (b) tripalmitin + commercial oleic acid systems; ■, melting temperature; ▲, eutectic temperature; left-pointing triangle, right-pointing triangle, × transitions in the solid phase. Solid lines represent the liquidus line and the eutectic temperature; dashed lines represent the probable boundaries between the solid solution region and the regions of solid−solid equilibrium (under the eutectic temperature) or SLE (above the eutectic temperature).

every obtained thermogram. This transition can be seen in the thermograms of Figure 5, especially in Figure 5d, and is represented in Figures 2b and 3 by the symbol ▲. In the thermograms of Figure 5 it can also be noted that the presence of linoleic acid interferes on the tristearin crystallization, since the exothermic peaks attributed to polymorphic transitions and recrystallization into the β-form no more occur for those mixtures in which $x_{\text{linoleic acid}} \geq 0.30$. In this last case only two endothermic peaks were observed; the first one, at the highest temperature, represents the complete melting of the sample (liquidus line), and the second one, at the lowest temperature, is attributed to the melting of a solid solution indicated by the left dashed line in Figure 2b.

The thermograms of both systems, tristearin + tripalmitin (Figure 4) and tristearin + linoleic acid (Figure 5), indicated that the last one exhibits less transitions beneath the liquidus line. The complexity of the tristearin + tripalmitin system can be related to the molecules that form this system, two triacylglycerols which already present a series of polymorphic transitions in their pure forms. Furthermore, these triacylglycerols have a small difference between their melting points, so that the SLE transition is concentrated in a restricted range of temperatures and a series of solid−solid transitions occur below that region. In the case of the other four systems at least one of the following conditions occurs: either the second component has a melting point significantly lower than the saturated triacylglycerols, or it is a fatty acid with a lower number of polymorphs. In fact, the number of transitions observed under the liquidus line decreased according to the second mixture component, be it an unsaturated triacylglycerol, a saturated fatty acid, or an unsaturated fatty acid, as can be seen in Figures 1, 2, and 3.

Although the studied systems show slightly different behaviors due to the transitions under the liquidus line, all systems seem to exhibit a solid solution at the extremity of the phase diagram rich in the heavier triacylglycerol. To confirm the occurrence of the solid solution in the phase diagrams, the enthalpy of the eutectic

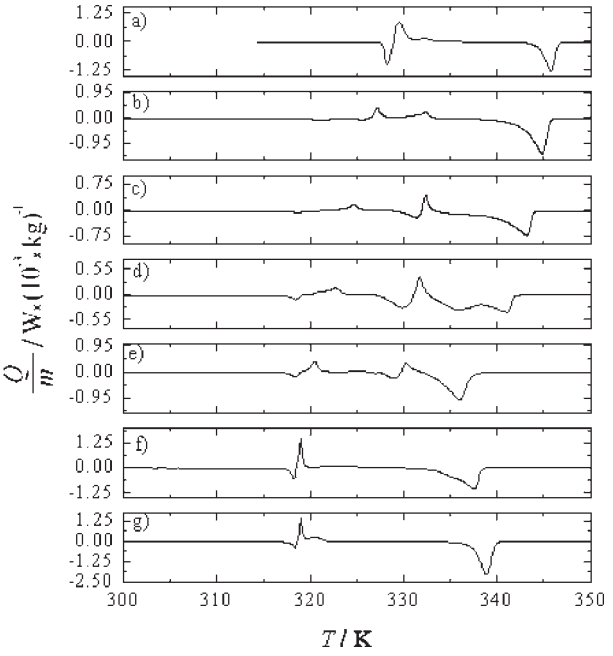

Figure 4. Thermograms of the tristearin + tripalmitin system: (a) $x_{\text{tripalmitin}} \cong 0.00$; (b) $x_{\text{tripalmitin}} \cong 0.10$; (c) $x_{\text{tripalmitin}} \cong 0.30$; (d) $x_{\text{tripalmitin}} \cong 0.50$; (e) $x_{\text{tripalmitin}} \cong 0.70$; (f) $x_{\text{tripalmitin}} \cong 0.90$; (g) $x_{\text{tripalmitin}} \cong 1.00$.

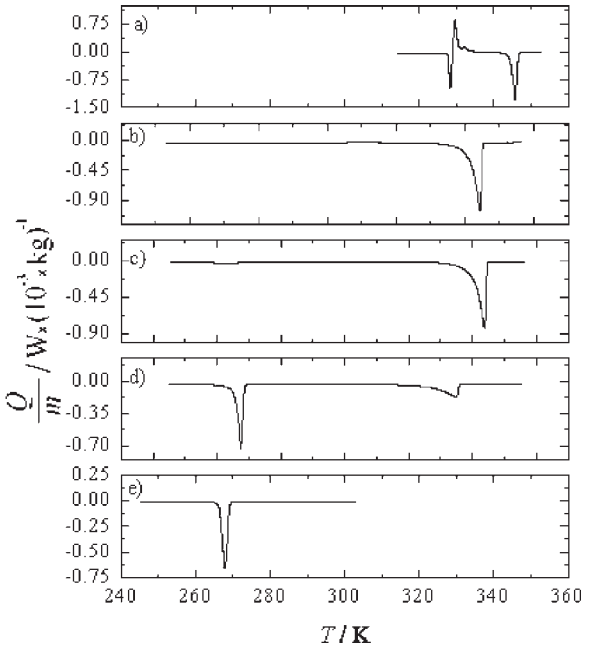

Figure 5. Thermograms of the tristearin + linoleic acid system: (a) $x_{\text{tripalmitin}} \cong 0.00$; (b) $x_{\text{tripalmitin}} \cong 0.30$; (c) $x_{\text{tripalmitin}} \cong 0.40$; (d) $x_{\text{tripalmitin}} \cong 0.90$; (e) $x_{\text{tripalmitin}} \cong 1.00$.

reaction was plotted as a function of each mixture composition (Tammann plot). This plot is presented in Figure 6 for the systems tristearin + tripalmitin and tristearin + linoleic acid. The enthalpy values were calculated by integration of the thermal curves using the *TA Universal Analysis* program. For a simple eutectic system the Tammann plot should present linearly increasing values of enthalpy until a maximum value, occurring exactly at the eutectic point concentration, and afterward enthalpy values that decrease linearly for higher compositions.[27] Via the Tammann plot it is possible to identify the concentration ranges of the two solid phase regions associated with the eutectic point.[27−29] As can be seen in Figure 6a, for the tristearin + tripalmitin system, this biphasic region does not extend to the pure tristearin side, indicating the occurrence of a solid solution at this extremity of the phase diagram. For compositions higher than the eutectic point, the Tammann plot of the tristearin + tripalmitin system also indicates the occurrence of a solid solution. In case of the tristearin + linoleic acid system (Figure 6b), the Tammann plot shows an increase in enthalpy with composition until the pure linoleic acid composition is reached. Therefore, a solid solution only occurs close to the pure tristearin extremity. In fact, for all of the binary mixtures studied in the present work, the formation of a solid solution is observed at least in the left side of the reported phase diagrams.

A further confirmation that these systems form solid solutions was obtained by optical microscopy. Optical images of the tristearin + tripalmitin system at $x_{\text{tripalmitin}} \cong 0.10$ are presented in Figure 7. According to the literature,[30] a simple eutectic system is divided in four equilibrium regions: two biphasic regions of SLE, one monophasic liquid region and one biphasic solid region. The SLE regions extend from the pure components to the eutectic composition and are delimited by the liquidus line and eutectic temperature. The monophasic liquid region, formed by both components after melting, is above the liquidus line, and a biphasic solid region, in which the two pure components coexist independently in a solid state, is below the eutectic temperature (solidus line). Obeying this description, if the tristearin + tripalmitin system behaved as a simple eutectic one, both solid and liquid phases should coexist for temperatures higher than the eutectic temperature, approximately 336 K. In Figure 7, at 331.15 K, approximately 5 K lower than the eutectic temperature, the whole sample is in a solid state, as expected. With the temperature increase to 343.45 K no change is observed in the images (Figures 7a−d). The presence of small amounts of liquid is noted only in Figure 7e, at 344.15 K, as indicated by the arrow in this figure. The existence of liquid is acknowledged by the round shape that the crystal border assumes and by the change in color; the sample became bright due to the new arrangement of the molecules. From this temperature (344.15 K) upward, the amount of liquid in the images increases until complete melting of the sample at 345.35 K, Figure 7i. These images indicate that the tristearin + tripalmitin system does not obey the description of a simple eutectic system, confirming the existence of a solid solution in the extremity of the phase diagram rich in the component with higher melting point, and in this way, they corroborate the prior results of the Tammann plot. According to the optical microscopy images, the eutectic reaction can be observed only for compositions equal or higher than $x_{\text{tripalmitin}} \cong 0.30$. The Tamman plot suggests that the eutectic reaction disappears close to the composition $x_{\text{tripalmitin}} \cong 0.20$. A better delimitation of this boundary requires further investigation around this composition range. Optical images were captured for all compositions of the tristearin + tripalmitin system, as presented in Figure 1. Both sets of data, obtained by the DCS and the optical microscopy, are in relatively good agreement, with average absolute deviations in the melting temperature and in the eutectic temperature lower than (0.95 and 0.65) K, respectively.

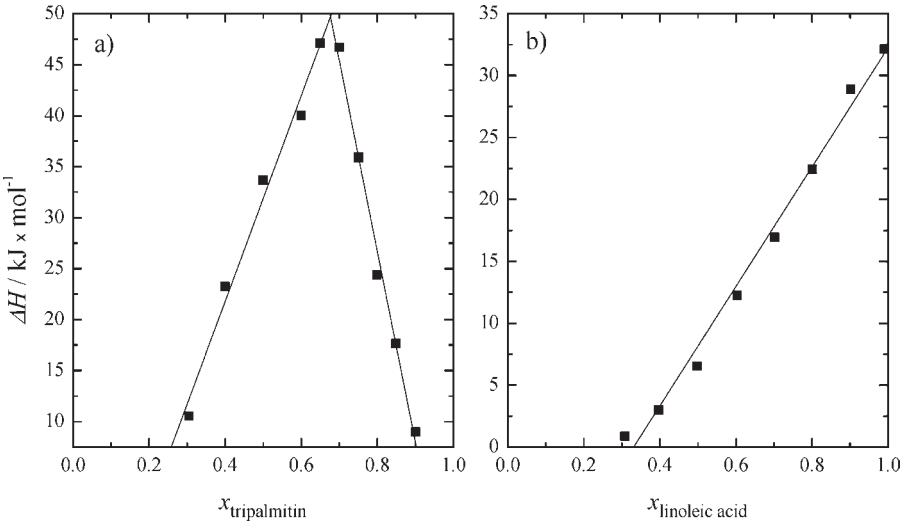

Figure 6. Tammann plots of the (a) tristearin + tripalmitin and (b) tristearin + linoleic acid systems; ■, enthalpy of the eutectic reaction; —, linear fit to the enthalpy values.

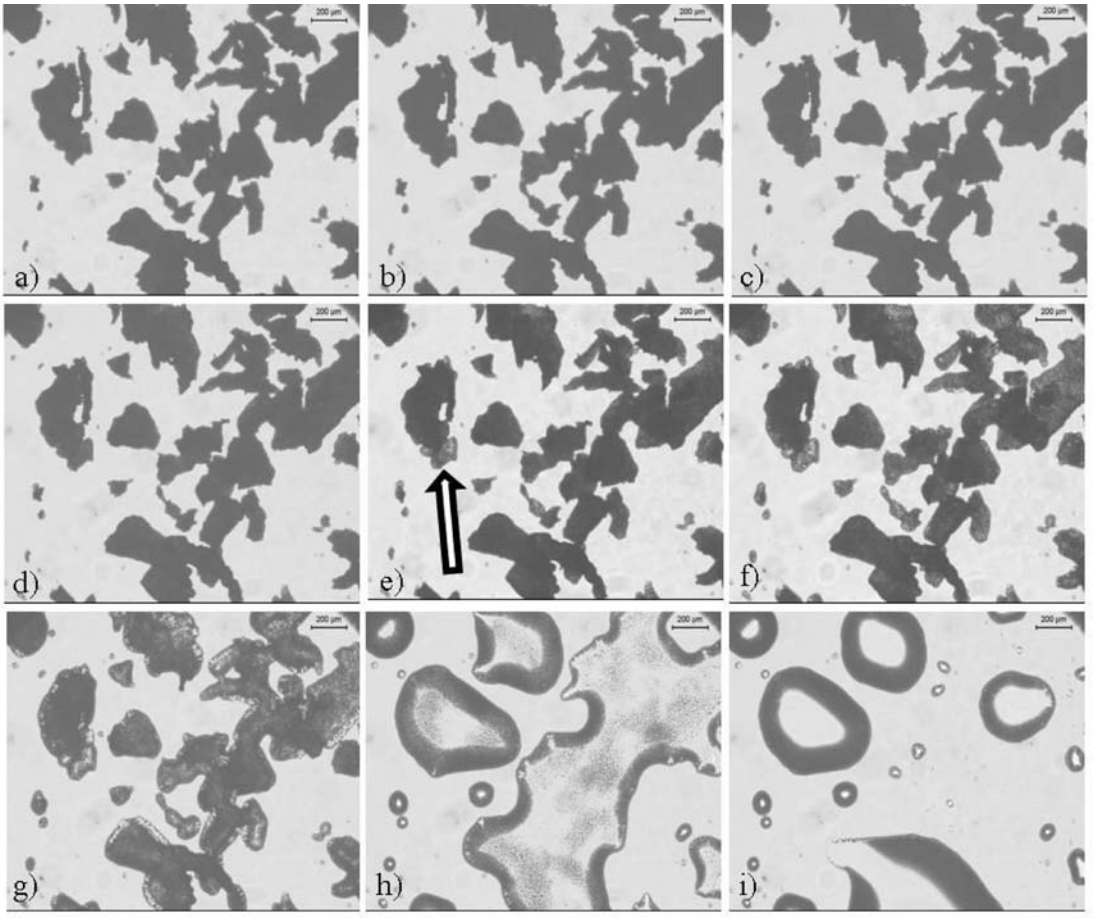

Figure 7. Optical images of the tristearin + tripalmitin system for $x_{tripalmitin} \cong 0.10$; (a) 331.15 K; (b) 333.15 K; (c) 343.15 K; (d) 343.75 K; (e) 344.15 K; (f) 344.35 K; (g) 344.55 K; (h) 344.95 K; (i) 345.35 K.

Equation 1 was used to describe the SLE, and this approach assumes that all systems behaved as simple eutectic ones.[12,31] The liquidus line of the multicomponent system formed by tripalmitin + commercial oleic acid was predicted using the UNIFAC model.[32] The liquidus line of the other four systems was modeled using the Margules-2-suffix, Margules-3-suffix, and

Table 7

model name	binary parameters	$RT \ln \gamma_i$
Margules-3-suffix	A_{ij} and A_{ji}	$[A_{ij} + 2(A_{ji} - A_{ij})x_i]x_j^2$; when $A_{ij} = A_{ji}$ the equation is called Margules 2-suffix
NRTL	g_{ij}, g_{jj} and g_{ji}, g_{ii}	$x_j^2[\tau_{ji}((G_{ji})/(x_i + x_jG_{ji}))^2 + ((\tau_{ij}G_{ij})/((x_j + x_iG_{ij})^2))]$ $\tau_{ij} = (\Delta g_{ij})/(RT)$; $\Delta g_{ij} = A_{0,ij} + A_{1,ij}T$; and $G_{ij} = \exp(-\alpha_{ij}\tau_{ij})$

Table 8. Deviations Obtained for the Margules-3-Suffix, Margules-2-Suffix, and NRTL Models

model	rmsd[a]				
	tristearin + tripalmitin	tristearin + palmitic acid	tristearin + linoleic acid	tripalmitin + triolein	tripalmitin + commercial oleic acid
Margules-3-suffix	0.52	0.16	0.22	0.10	
Margules-2-suffix	0.73	0.36	0.71	0.40	
NRTL ($\alpha_{12} = 0.30$)	0.57	0.15	0.22	0.37	
UNIFAC	1.42	0.46	0.92	0.57	0.79

[a] rmsd = $(\sum_{i=1}^{n}(T_{i,\mathrm{exp}} - T_{\mathrm{i,calc}})^2/n)^{1/2}$, where T is temperature and n is the number of experimental points.

Table 9. Adjustment Parameters Obtained by the Margules-3-Suffix, Margules-2-Suffix, and NRTL Models

system	Margules-3-suffix		NRTL ($\alpha_{12} = 0.30$)		Margules-2-suffix
	A_{12}/J·mol^{-1}	A_{21}/J·mol^{-1}	Δg_{12}/J·mol^{-1}	Δg_{21}/J·mol^{-1}	A_{12}/J·mol^{-1}
tristearin + tripalmitin	−111211.22	−7528.36	4506.65	−5770.67	−2915,63
tristearin + palmitic acid	1388.68	−710.40	−3721.25	7908.08	191.25
tristearin + linoleic acid	3017.29	−112.96	−3199.30	9471.07	753.13
tripalmitin + triolein	643.90	−1448.26	1925.32	−2083.14	−552.34

NRTL models[33] and also predicted using the UNIFAC model. The model equations used are presented in Table 7.

$$ln\left(\frac{1}{x_i^l\gamma_i^l}\right) = \frac{\Delta H_{i,\mathrm{fus}}}{RT_{i,\mathrm{fus}}}\left(\frac{T_{i,\mathrm{fus}}}{T} - 1\right) \quad (1)$$

Considering the ideal behavior of the solid phase, as mentioned before, the liquidus line was well-described, with low average deviations between experimental and calculated values (Table 8), but the existence of solid solutions in the extremes of the phase diagrams was not considered in the modeling approach. All of the adjusted parameters are presented in Table 9. The best modeling results were obtained using the Margules-3-suffix and NRTL models. In the case of the predictive UNIFAC model the deviations are larger, but considering that no further adjustment was done to represent the nonideality of the liquid phase, the results were also good.

CONCLUSION

SLE data of tristearin + palmitic acid, tristearin + tripalmitin, tristearin + linoleic acid, tripalmitin + triolein, and tripalmitin + commercial oleic acid systems were successfully determined by the DSC technique. The Tammann plot and images obtained by optical microscopy confirm the occurrence of solid solutions at the extremity of the phase diagram rich in the component with higher melting temperature. The best modeling of the equilibrium data was obtained by the Margules-3-suffix model. The UNIFAC model predicted in an appropriate way the liquidus line of the system formed by tripalmitin + commercial oleic acid.

AUTHOR INFORMATION

Corresponding Author

*Antonio José de Almeida Meirelles, Department of Food Engineering (DEA), Faculty of Food Engineering (FEA), University of Campinas (UNICAMP). CEP: 13083-862. Campinas, São Paulo, Brazil. Phone: +55-19-3251-4037, e-mail: tomze@fea.unicamp.br.

Funding Sources

The authors are grateful to CNPq (480992/2009-6 and 304495/2010-7), FAPESP (08/09502-0, 08/56258-8), CAPES, and FAEPEX/UNICAMP for their financial support.

REFERENCES

(1) Bailey, A. E. *Melting and solidification of fats*; Interscience Publishers: New York, 1950.

(2) Müller, E.; Stage, H. *Experimentelle vermessung von dampf-flüssigkeits-phasengleichgewichten*; Springer: Berlin, 1961.

(3) Domanska, U.; Domanski, K.; Klofutar, C.; Paljk, S. Excess-Enthalpies of Nonan-1-ol and Undecan-1-ol with Octane at High Dilutions and at 298.15 K. *Thermochim. Acta* **1990**, *164*, 227–236.

(4) Hofman, T.; Domanska, U. Solubilities of normal alkanoic acids by the UNIFAC group contribution method. *J. Solution Chem.* **1988**, *17* (3), 237–248.

(5) Domanska, U.; Rolinska, J. *Solid-liquid equilibrium data collection organic compounds monocarboxylic acids*; PWN-Polish Scientific Publishers: Warszawa, 1988.

(6) Boodhoo, M. V.; Bouzidi, L.; Narine, S. S. The binary phase behavior of 1,3-dicaproyl-2-stearoyl-sn-glycerol and 1,2-dicaproyl-3-stearoyl-sn-glycerol. *Chem. Phys. Lipids* **2009**, *157* (1), 21–39.

(7) Boodhoo, M. V.; Kutek, T.; Filip, V.; Narine, S. S. The binary phase behavior of 1,3-dimyristoyl-2-stearoyl-sn-glycerol and 1,2-dimyristoyl-3-stearoyl-sn-glycerol. *Chem. Phys. Lipids* **2008**, *154* (1), 7–18.

(8) Costa, M. C.; Sardo, M.; Rolemberg, M. P.; Coutinho, J. A. P.; Meirelles, A. J. A.; Ribeiro-Claro, P.; Krähenbühl, M. A. The solid-liquid phase diagrams of binary mixtures of consecutive, even saturated fatty acids. *Chem. Phys. Lipids* **2009**, *160*, 85–97.

(9) Costa, M. C.; Sardo, M.; Rolemberg, M. P.; Coutinho, J. A. P.; Meirelles, A. J. A.; Ribeiro-Claro, P.; Krähenbühl, M. A. The solid−liquid phase diagrams of binary mixtures of consecutive, even saturated fatty acids: differing by four carbon atoms. *Chem. Phys. Lipids* **2009**, *157*, 40–50.

(10) Costa, M. C.; Boros, L. A. D.; Rolemberg, M. P.; Krahenbuhl, M. A.; Meirelles, A. J. A. Solid−Liquid Equilibrium of Saturated Fatty Acids plus Triacylglycerols. *J. Chem. Eng. Data* **2010**, *55* (2), 974–977.

(11) Costa, M. C.; Krähenbühl, M. A.; Meirelles, A. J. A.; Daridon, J. L.; Pauly, J.; Coutinho, J. A. P. High pressure solid-liquid equilibria of fatty acids. *Fluid Phase Equilib.* **2007**, *253* (2), 118–123.

(12) Costa, M. C.; Rolemberg, M. P.; Boros, L. A. D.; Krähenbühl, M. A.; Oliveira, M. G.; Meirelles, A. J. A. Solid-liquid equilibrium of binary fatty acids mixtures. *J. Chem. Eng. Data* **2007**, *52*, 30–36.

(13) Costa, M. C.; Rolemberg, M. P.; dos Santos, A. O.; Cardoso, L. P.; Krahenbuhl, M. A.; Meirelles, A. J. A. Solid-Liquid Equilibrium of Tristearin with Refined Rice Bran and Palm Oils. *J. Chem. Eng. Data* **2010**, *55* (11), 5078–5082.

(14) Costa, M. C.; Rolemberg, M. P.; Meirelles, A. J. A.; Coutinho, J. A. P.; Krahenbuhl, M. A. The solid-liquid phase diagrams of binary mixtures of even saturated fatty acids differing by six carbon atoms. *Thermochim. Acta* **2009**, *496* (1−2), 30–37.

(15) Moreno, E.; Cordobilla, R.; Calvet, T.; Cuevas-Diarte, M. A.; Gbabode, G.; Negrier, P.; Mondieig, D.; Oonk, H. A. J. Polymorphism of even saturated carboxylic acids from n-decanoic to n-eicosanoic acid. *New J. Chem.* **2007**, *31*, 947–957.

(16) Oh, J. H.; McCurdy, A. R.; Swanson, B. G. Characterization and thermal stability of polymorphic forms of synthesized tristearin. *J. Food Sci.* **2002**, *67* (8), 2911–2917.

(17) Matovic, M.; van Miltenburg, J. C.; Los, J.; Gandolfo, F. G.; Floter, E. Thermal properties of tristearin by adiabatic and differential scanning calorimetry. *J. Chem. Eng. Data* **2005**, *50* (5), 1624–1630.

(18) Kellens, M.; Meeussen, W.; Gehrke, R.; Reynaers, H. Synchrotron Radiation Investigations of the Polymorphic Transitions of Saturated Monoacid Triglycerides. 1. Tripalmitin and Tristearin. *Chem. Phys. Lipids* **1991**, *58* (1−2), 131–144.

(19) Kellens, M.; Meeussen, W.; Hammersley, A.; Reynaers, H. Synchrotron Radiation Investigations of the Polymorphic Transitions in Saturated Monoacid Triglycerides. 2. Polymorphism Study of a 50−50 Mixture of Tripalmitin and Tristearin during Crystallization and Melting. *Chem. Phys. Lipids* **1991**, *58* (1−2), 145–158.

(20) MacNaughtan, W.; Farhat, I. A.; Himawan, C.; Starov, V. M.; Stapley, A. G. F. A differential scanning calorimetry study of the crystallization kinetics of tristearin-tripalmitin mixtures. *J. Am. Oil Chem. Soc.* **2006**, *83* (1), 1–9.

(21) Norton, I. T.; Leetuffnell, C. D.; Ablett, S.; Bociek, S. M. A Calorimetric, NMR and X-Ray-Diffraction Study of the Melting Behavior of Tripalmitin and Tristearin and Their Mixing Behavior with Triolein. *J. Am. Oil Chem. Soc.* **1985**, *62* (8), 1237–1244.

(22) AOCS. *Official methods and recommended practices of the American Oil Chemists' Society*, 3rd ed.; AOCS: Champaign, IL, 1988; Vols. 1−2.

(23) Hartman, L.; Lago, R. C. A. Rapid Preparation of Fatty Acid Methyl Esters from Lipids. *Lab. Pract.* **1973**, *22*, 475–476.

(24) Rodrigues, C. E. C.; Antoniassi, R.; Meirelles, A. J. A. Equilibrium data for the system rice bran oil plus fatty acids plus ethanol plus water at 298.2 K. *J. Chem. Eng. Data* **2003**, *48* (2), 367–373.

(25) Boros, L.; Batista, M. L. S.; Vaz, R. V.; Figueiredo, B. R.; Fernandes, V. F. S.; Costa, M. C.; Krahenbuhl, M. A.; Meirelles, A. J. A.; Coutinho, J. A. P. Crystallization Behavior of Mixtures of Fatty Acid Ethyl Esters with Ethyl Stearate. *Energy Fuels* **2009**, *23*, 4625–4629.

(26) Costa, M. C.; Rolemberg, M. P.; Santos, A. O. d.; Cardoso, L. P.; Krähenbühl, M. A.; Meirelles, A. J. A. Solid-Liquid Equilibrium of Tristearin with Refined Rice Bran and Palm Oils. *J. Chem. Eng. Data* **2011**in press.

(27) Chernik, G. G. Phase-Equilibria in Phospholipid Water-Systems. *Adv. Colloid Interface Sci.* **1995**, *61*, 65–129.

(28) Inoue, T.; Hisatsugu, Y.; Ishikawa, R.; Suzuki, M. Solid-liquid phase behavior of binary fatty acid mixtures 2. Mixtures of oleic acid with lauric acid, myristic acid, and palmitic acid. *Chem. Phys. Lipids* **2004**, *127* (2), 161–173.

(29) Inoue, T.; Hisatsugu, Y.; Suzuki, M.; Wang, Z.; Zheng, L. Solid-liquid phase behavior of binary mixtures 3. Mixtures of oleic acid with capric acid (decanoic acid) and caprylic acid (octanoic acid). *Chem. Phys. Lipids* **2004**, *132*, 225–234.

(30) Nývlt, J. *Solid-liquid phase equilibria*; Elsevier: Amsterdam, 1977.

(31) Costa, M. C.; Boros, L. A. D.; Rolemberg, M. P.; Krähenbühl, M. A.; Meirelles, A. J. A. Solid-liquid equilibrium of saturated fatty acids + triacylglycerols. *J. Chem. Eng. Data* **2009**, *55* (2), 974–977.

(32) Hansen, H. K.; Rasmussen, P.; Fredenslund, A.; Schiller, M.; Gmehling, J. Vapor-Liquid-Equilibria by Unifac Group Contribution 5. Revision and Extension. *Ind. Eng. Chem. Res.* **1991**, *30* (10), 2352–2355.

(33) Walas, S. M. *Phase equilibria in chemical engineering*; Butterworth: Stoneham, 1984.